# Novel Pentagonal Dual-Mode Filters with Adjustable Transmission Zeros

**Zhaojun Zhu, Shuo Liang, and Chaolei Wei**

Institute of Applied Physics
University of Electronic Science and Technology of China, Chengdu, 610054, China
uestc98@163.com, uestcliangshuo@163.com, uestcweichaolei@163.com

***Abstract*** **─** Novel compact pentagonal dual-mode filters with open stub is presented. The field patterns of this type of resonators are investigated using full-wave electromagnetic simulations. The technique of utilizing capacitive and inductive source-load coupling to improve the performance of filters is explored. Advantages of using this type of filter are not only its compact size, but also its transmission zeros that can be independently controlled. Then, two dual-mode bandpass filters are designed, fabricated and tested to validate the design concept. Both simulated and measured results are presented.

***Index Terms*** **─** Bandpass filter, dual-mode, transmission zero.

## I. INTRODUCTION

Bandpass filter (BPF) is one of the most important components in microwave circuits. To meet the requirement of modern microwave communication systems, microwave BPFs with compact size and high performance are in demand. The dual-mode resonators are attractive because each resonator can be used as a doubly tuned circuit, and therefore, the number of resonators is reduced by half, resulting in a compact size. Wolff first demonstrated a microstrip dual-mode filter in 1972 [1]. Since then, dual-mode microstrip filters have been widely used in communications systems [2-3]. Among them, E-shaped microstrip resonators and filters have been originally reported in [4]. More recently, the E-shaped resonator was modeled as a dual-mode resonator in [5]. However, it was difficult to control the location of the transmission zeros. Circular dual-mode filter based on source-load coupling was proposed in [6]. By introducing a capacitive cross-coupling between the input and output ports so that additional zero can be generated, but transmission zeros cannot be independently controlled. The open stub dual-mode filter with adjustable transmission zeros by inductive source-load coupling (S-L coupling) was firstly proposed in [8]. Two novel bandpass filters with multiple transmission zeros using only four open/ shorted stubs was proposed in [9]. The out-of-band transmission zeros can be adjusted easily by only changing the electrical length of the four open/shorted stub. But the resonator occupied a large circuit area, size reduction is becoming a major design consideration for practical applications.

In this paper, two compact bandpass filters with a pentagonal dual-mode resonator and S-L coupling are introduced. The reduction of the size is achieved by using a pentagonal dual-mode resonator. Furthermore, with a cross-coupling between the input and output feed lines, two tunable transmission zeros are obtained that can be controlled independently by the amount of the capacitive or inductive S-L coupling. The proposed bandpass filter shows a good stopband rejection because of the two tunable transmission zeros. Two exemplary filters verify the feasibility of the technique.

## II. DUAL-MODE PENTAGONAL RESONATOR

Figure 1 shows the geometry of proposed dual-mode filters with the pentagonal open-loop resonator by open stub loaded. The filter comprises an improved pentagonal half-wavelength resonator and a hexagonal open loaded stub. The S-L coupling include two types, i.e., capacitive and inductive S-L coupling.

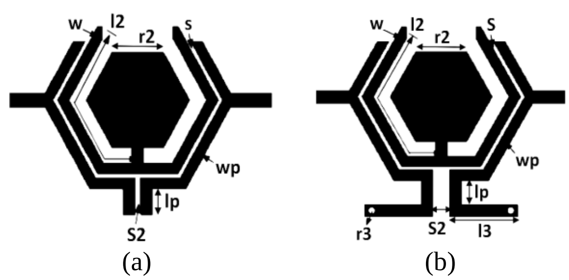


Fig. 1. Layout of the proposed pentagonal dual-mode bandpass filter: (a) capacitive S-L coupling, and (b) inductive S-L coupling.

Figure 2 shows a T-shaped resonator model with a half-wavelength resonator and a shunt open stub, where $z_1$ is the characteristic impedance of the half-

*Submitted On: August 15, 2014*
*Accepted On: August 11, 2016*

wavelength resonator with the electrical length $\theta_1 = 90^\circ$, and $z_2$ the characteristic impedance of the open stub with electrical length $\theta_2$. $C_1$ is the coupling capacitance between resonator and feed line. As $\theta_2$ increases, the odd resonant frequencies are fixed, while the even resonant frequencies and the transmission zero frequency keeps decreasing. When $\theta_2$ is slightly smaller/larger than $90^\circ$, the even resonant frequency is slightly beyond/below fundamental frequency of the half-wavelength resonator, respectively. The proposed resonator then becomes a dual-mode resonator with a transmission zero close to the resonant frequency [7]. If the S-L coupling is introduced, an additional transmission zero is presented. Then, the proposed filter will show two transmission zeros.

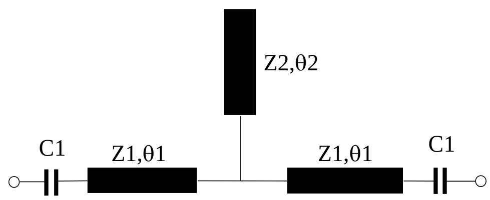


Fig. 2. Schematic of a half-wavelength resonator with an open stub.

For a compact size, the half-wavelength length line is bent to a pentagon, and the uniform shunt open stub is also replaced by a hexagonal stepped-impedance open stub. The open hexagonal stub at the centre of the half-wavelength resonator introduces another transmission pole near the fundamental frequency. This new pole and the fundamental frequency pole of the half-wavelength resonator make the proposed structure a dual-mode resonator. So this symmetric structure can support two modes, i.e., an even mode and odd mode.

The commercially available full-wave electromagnetic simulators (HFSS) were used to characterize the electric field patterns for a dual-mode open-loop resonator. HFSS uses the finite element method (FEM) to analyze the electromagnetic characteristics of 3D objects. The basic process of solving the problem by FEM includes three parts, which are the mesh discretization of the object, the solution of the simultaneous matrix equations related the mesh and the postprocessing calculation of the problem.

It can be seen that the whole structure is symmetrical with the center point, so the center point is modeled as the origin point and the mirror operation is applied. The physical excitation of the filter is by the coaxial line with the TEM wave. In order to use the wave-guide port in the simulation code, the port surface must cover more than ninety-five percent of the TEM field. It is assumed that the width of the excitation microstrip is w and the thickness of the dielectric layer is h. The height of the wave port is generally set to 6~10h. When w>h, the width of the wave port is set to about 10w; when w<h, the width of the wave port is set to about 5w. Finally, the height and width of the wave port of are 10h and 10w in this paper.

According to the standard which is set up by user, HFSS simulation code uses adaptive mesh generation technology. The solution frequency of the meshing is generally set at the center frequency of the filter. After each new mesh subdivision, HFSS will compare the results of the S parameters with the old one. If the error is less than the set criterion, it is shown that the result is convergent and the adaptive process will end. The dimensions are optimized by a full-wave simulation to take all the discontinuities into consideration.

Figure 3 depicts the simulated electric field vector between the metal strip and ground plane at the resonance frequency. The electric field pattern of the odd mode is illustrated in Fig. 3 (a), where the maxima of the field are located along the left and right arms. The field distribution is similar to that of a half-wavelength single-mode resonator. As a consequence, the open stub does not affect the resonant frequency of the odd mode. Figure 3 (b) shows the electric field pattern of the even-mode, where the maxima of the field are moved to the open stub and both side of the arms. Moreover, it is observed from the direction of the electric field vector that the field is symmetric with respect to the symmetry axis. Hence, changing the dimension of the open stub makes the resonant frequency of the even mode shift.

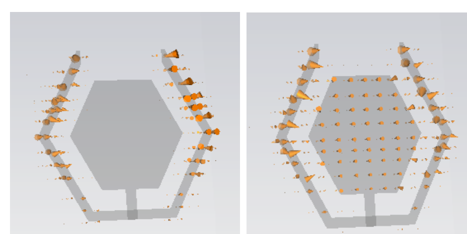

(a) (b)

Fig. 3. Simulated electric field patterns for a dual-mode pentagonal open-loop resonator: (a) odd mode and (b) even mode.

To observe the mode splitting, the dual-mode pentagonal loop resonators have been simulated with different loaded element size. The resonant frequencies of the two modes are plotted in Fig. 4 as a function of the size $l_2$ and $r_2$. As shown in Fig. 4 (a), when $l_2$ increases from 10 to 20 mm, the resonant frequency of the odd mode decreases from 4.45 to 2.8 GHz, while that of the even mode decreases from 3.85 to 3.1 GHz. As shown in Fig. 4 (b), when $r_2$ increases from 3 to 5 mm, the resonant frequency of the even mode decreases from 3.58 to 3.45 GHz, while that of the odd mode hardly change.

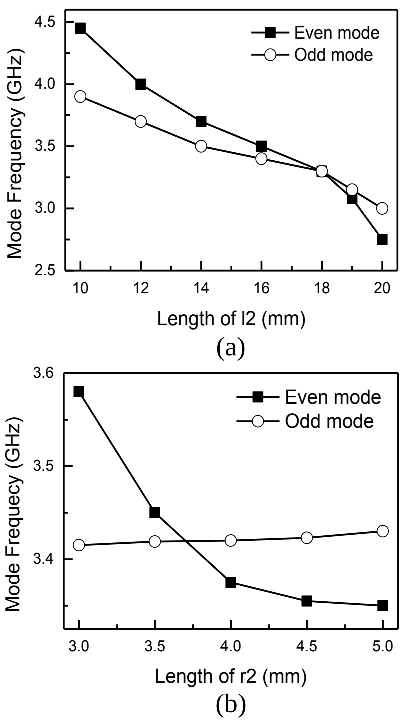


Fig. 4. Simulated resonance frequencies of the two modes against: (a) $l_2$, where $r_2$ = 5 mm, and (b) $r_2$, where $l_2$ = 15 mm.

## III. BANDPASS FILTERS USING DUAL-MODE PENTAGONAL RESONATOR

Figure 1 shows the layout of the pentagonal dual-mode open loop BPF. It consists of the capacitive S-L coupling and inductive S-L coupling filter. The gap between the resonator and coupling arms was selected in consideration of strong coupling and etching tolerance. The characteristic impedance of the input/output microstrip is taken as 50 ohm. The length of the S-L coupling line is $l_p$. The gap of the S-L coupling line is $s_2$.

As illustrated in [6], the open stub dual-model filter has an interesting property. There is an inherent finite-frequency transmission zero when the two modes split. If $f_{even} < f_0 < f_{odd}$, the inherent transmission zero would be in the lower stopband. If $f_{odd} < f_0 < f_{even}$, the inherent transmission zero would be in the upper stopband. $f_0$ is the center frequency.

For further improving the filters' performance, S-L coupling is introduced to generate an additional zero. Using capacitive and inductive S-L coupling technique, the response with two adjustable zeros can be obtained for the proposed dual-mode filters. The locations of these two transmission zeros can be controlled by transforming the type and amount of the source-load cross-coupling. For the capacitive S-L coupling, an additional transmission zero shows in the upper stopband. For the inductive S-L coupling, an additional transmission zero shows in the lower stopband. Two exemplary filters verify the feasibility of the new technique. We take $f_{odd} < f_0 < f_{even}$ for instance.

### A. Dual-mode filter with capacitive S-L coupling

Filter A exhibits both the inherent transmission zero and the additional zero in the upper stopband. Here, the capacitive S-L coupling is introduced to generate the additional zero. The locations of the additional zero may be controlled by adjusting the values of the $s_2$ and $l_p$. As shown in Fig. 5, when $s_2$ decreases from 1.1 to 0.7 mm, the inner transmission zero almost doesn't change, and the outer transmission zero moves toward the passband edge. As shown in Fig. 6, when $l_p$ increases from 1 to 2.4 mm, the inner transmission zero almost doesn't change, while the outer transmission zero moves toward the passband edge. Therefore, the $s_2$ and $l_p$ can be selected to meet the required filter selectivity.

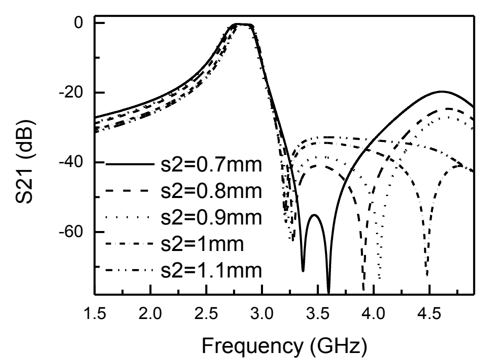


Fig. 5. Simulated scattering parameters of the filter A for five values of $s_2$.

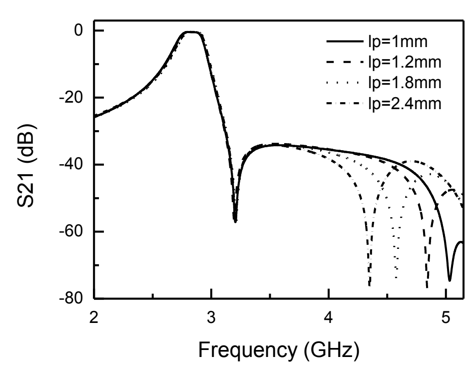


Fig. 6. Simulated scattering parameters of the filter A for four values of $l_p$.

The dimensions are optimized by a full-wave simulator to take all the discontinuities into consideration. The designed filter is fabricated on the substrate Rogers RO4003, which relative dielectric constant is 3.38 and the thickness is 0.508 mm. Figure 7 shows the photograph of the fabricated filter A. Both measured and simulated results are plotted in Fig. 8. As seen from the measured results, at the center frequency of 2.75 GHz, the 3 dB fractional bandwidth is about 8%. Two transmission zeros are realized at 3.2 and 4.75 GHz. The insertion loss is less than 2 dB in passband, and the minimum of insertion loss is 1.5 dB. The return loss is greater than 20 dB in passband. Simulation results almost agree with the measured results.

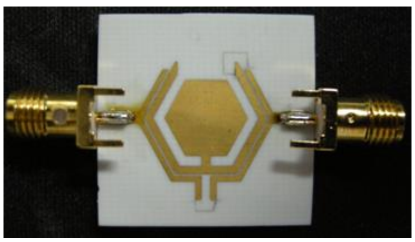

Fig. 7. Photograph of the fabricated filter A. Geometric parameters of the filters are $w$ =1, $r_2$ = 5, $l_2$ = 11.55, $l_p$ = 2, $s_2$ = 1 and $s$ = 0.22. All are in mm.

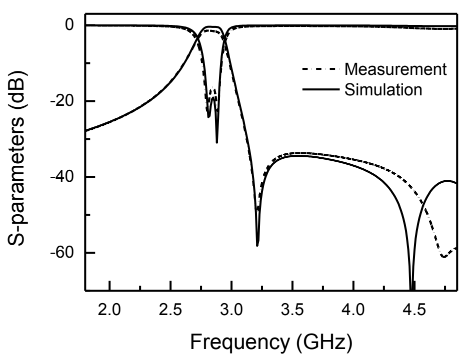


Fig. 8. Simulated and measured frequency responses of the filter A.

**B. Dual-mode filter with inductive S-L coupling**

Filter B demonstrates a filter characteristic with the inherent finite frequency zero located at the upper side of the passband, while the additional zero at the lower side. This is because $f_{odd} < f_0 < f_{even}$ for the proposed filter. As it has been noted, the inherent zero is at upper side of passband. The inductive S-L coupling is introduced to generate an additional zero at lower side of passband. As shown in Fig. 9 and Fig. 10, when $s_2$ decreases from 3.5 to 0.5 mm, the inherent transmission zero changed little, while the additional transmission zeros increases from 0.85 to 1.9 GHz. When $l_p$ increases from 1 to 7 mm, the inherent transmission zero also changed little, while the additional transmission zeros increases from 0.85 to 1.65 GHz. Thus, a sharper fall-off at both lower and upper passband edge may be achieved by adjusting the $s_2$ and $l_p$.

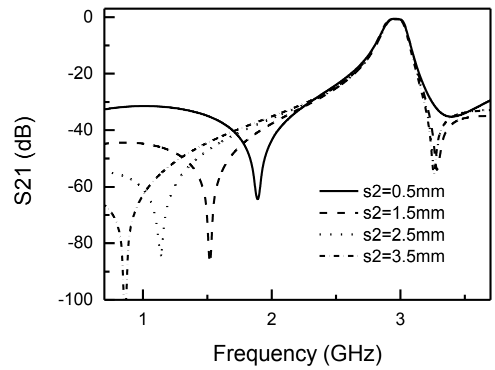


Fig. 9. Simulated scattering parameters of the filter B for four values of $s_2$.

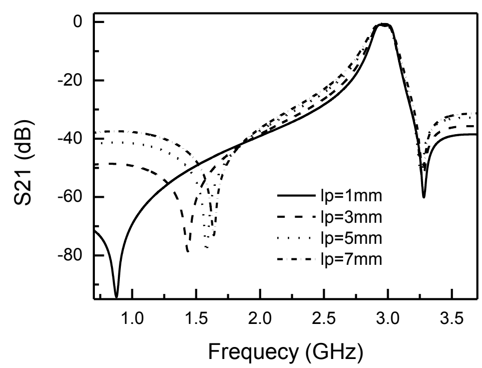


Fig. 10. Simulated scattering parameters of the filter B for four values of $l_p$.

Figure 11 shows the photograph of the fabricated filter B. The simulated and measured frequency responses are shown in Fig. 12. The simulated results show that the filter B operated at 3 GHz and a 3 dB fractional bandwidth of 5.3%. Two transmission zeros are located at 1.55 GHz and 3.3 GHz respectively. The minimum insertion loss is about 0.6 dB, and the return loss is greater than 20 dB in passband. The measured minimum insertion loss is about 2 dB, and the return loss is greater than 16 dB in passband. The measured results meet the simulation results well.

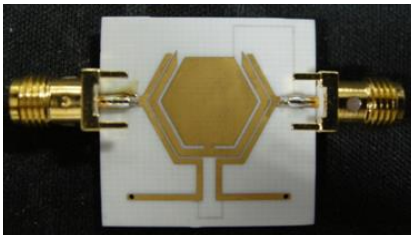

Fig. 11. Photograph of the fabricated filter B. Geometric parameters of the filters are $w$ =1, $r_2$ = 5, $r_3$ = 8, $l_2$ = 11.55, $l_3$ = 8, $l_p$ = 4, $s_2$ = 1.5 and $s$ = 0.18. All are in mm.

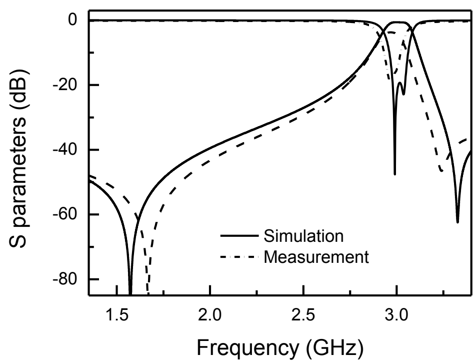


Fig. 12. Simulated and measured frequency responses of the filter B.

## IV. CONCLUSION

The application of capacitive and inductive S-L coupling has been studied intensively in this paper. The novel pentagonal dual-mode filter loaded by hexagonal open stub is presented. By S-L coupling, the proposed filters exhibits two transmission zeros. It reveals that a quasi-elliptic response with two adjustable transmission zeros can be obtained easily. The proposed structure and design method is verified by two exemplary filters.

## ACKNOWLEDGMENT

This work is supported by “National Natural Science Foundation of China (Grant No. 61101042)”.

## REFERENCES

[1] I. Wolff, “Microstrip bandpass filter using degenerate modes of a microstrip ring resonator,” *Electron. Lett.*, vol. 8, pp. 302-303, June 1972.

[2] B. F. Ganji and M. Samadbeik, “Simple configuration low-pass filter with very wide stop band,” *ACES Express Journal*, vol. 1, no. 1, pp. 4-7, 2016.

[3] X. Deng and K. D. Xu, “Novel microstrip ultra-wideband bandpass filter using radial-stub-loaded structure,” *ACES Express Journal*, vol. 1, no. 1, pp. 20-23, 2016.

[4] J. R. Lee and J. H. Cho, “New compact bandpass filter using microstrip λ/4 resonator with open stub inverter,” *IEEE Microw. Guided Wave Lett.*, vol. 10, no. 12, pp. 526-527, Dec. 2000.

[5] T. Yan, X. H. Tang, and J. Wang, “A novel quad-band bandpass filter using short stub loaded E-shaped resonators,” *IEEE Microwave & Wireless Components Letters*, vol. 25, no. 8, pp. 508-510, Aug. 2015.

[6] W.-H. Wu, “Compact double-mode cross-coupled microstrip bandpass filter with tunable transmission zeros,” *IET Microw. Antennas Propag.*, vol. 2, no. 4, pp. 373-377, Dec. 2008.

[7] L. Gao and X. Y. Zhang, “High-selectivity dual-band bandpass filter using a quad-mode resonator with source-load coupling,” *IEEE Microwave & Wireless Components Letters*, vol. 23, no. 9, pp. 474-476, Sept. 2013.

[8] J.-S. Hong and H. Shaman, “Dual-mode microstrip open-loop resonators and filters,” *IEEE Trans. Microw. Theory Tech.*, vol. 55, no. 8, pp. 1764-1770, Aug. 2007.

[9] W. Feng, X. Gao, and W. Che, “Bandpass filters with multiple transmission zeros using open/ shorted stubs,” *IET Microw., Antennas Propag.*, vol. 9, no. 8, pp. 769-774, June 2015.

[10] B. Yu, B. Jia, and Z. Zhu, “Compact tri-band bandpass filter with stub-loaded stepped-impedance resonator,” *Electron. Lett.*, vol. 51, no. 9, pp. 701-703, Apr. 2015.

**Zhaojun Zhu** was born in Sichuan, China, in 1978. He received the B.S. degree and the Ph.D. degree in Physical Electronics in UESTC, Chengdu, in 2002 and 2007 respectively. Since 2012, he has been an Associate Professor with the UESTC. His research interests include the design of microwave and millimeter-wave circuits.

**Shuo Liang** was born in SiChuan Province, China, in 1990. He received the B.S. degree in School of Electronic Engineering from HUAT, Hubei, in 2014, and is currently working toward the M.D. degree in UESTC. His research interests include the design of microwave and millimeter-wave circuits.

**Chaolei Wei** was born in Shandong Province, China, in 1981. He received the B.S. degree in Physics from the Liaocheng University, in 2006, and the M.D. degree in Nuclear Energy Engineering from the Institute of Southwest Physics, in 2009, respectively, and is currently working toward the Ph.D. degree in UESTC. His research interests include the design of microwave and millimeter-wave circuits.